Visual Guidance for a Spatial Discrepancy Problem of in Encountered-Type Haptic Display

Chang-Gyu Lee, Gregory Lynn Dunn, Ian Oakley, and Jeha Ryu, *Member, IEEE*

***Abstract*—In virtual environments, spatial discrepancies between visual and haptic scenes negatively impact user performance and experience. This paper shows how spatial discrepancies due to pose differences can occur in a haptic augmented virtuality system with an encountered-type haptic display. To mitigate this problem, we propose visual guidance, an algorithm that dynamically manipulates the visual scene to compensate for discrepancies. The effectiveness of this algorithm was verified in a pair of studies involving a button pressing task and spatial discrepancies between ±150 mm and ±40°. Experimental results show that discrepant trials using the technique yield error rates and a number of speed peaks (representing the number of targeting movements) that are comparable to those attained in trials with zero spatial discrepancy. This result was also achieved without requiring a dedicated adaptation or training process, ensuring the algorithm can be used immediately by users. A pair of follow-up studies also indicates the algorithm has little impact on subjective ratings of simulator sickness, suggesting that sporadic use of the algorithm will not negatively affect user's experience of a virtual environment. We believe that the visual guidance algorithm presented in this paper can be used to create more useful and compelling experiences in various haptic training applications incorporating encountered-type haptic displays.**

***Index Terms*—Encountered-type haptic display, haptic augmented virtuality (HAV), performance evaluation, spatial discrepancy, visual guidance.**

I. Introduction

HAPTIC virtual reality (VR) training [1] provides many benefits. In contrast to real-world training, it is safe as trainee error cannot result in injury or damage. Compared to training on physical mock-ups [2], it is adaptable: changes can be made easily by modifying virtual contents. Furthermore, after initial investments in display hardware, it is relatively cheap. Generally, in order to develop such haptic VR training, a precise and robust motion tracking is required [3]. However, haptic VR training is not without problems. A recurring issue is the plausibility, or physical realism, of contact cues in the training environment—with most current haptic solutions, force feedback is applied through a single proxy object, most typically a stylus, gripper, or bespoke tool (e.g., a laparoscopic surgical instrument [1]), or via an exoskeletal system [4]. While these approaches can be effective in simple single tool scenarios, many realistic training simulations involve use of multiple, spatially distributed objects or devices. For example, in plant safety training, an operator typically interacts with a set of tools of various sizes and types (e.g., the buttons, valves, and levers in Fig. 1) set at different poses (positions and orientations). In such a scenario, a realistic haptic experience can only be created by mimicking both tactile and force/torque cues of all the different tools.

One way of achieving this goal is extending Milgram *et al.*'s [5] notion of augmented virtuality or "*introducing real objects into the principally (virtual) graphic world*" to include tactile and force/torque cues. We term this approach haptic augmented virtuality (HAV) and suggest it can be achieved by combining traditional force feedback cues with real tools in an encountered-type haptic system [6], [7]. In such a system, a robotic device presents haptic cues only in appropriate poses in virtual environments. When no cues should be present, it moves away from the hand, allowing free movement. Such systems can be equipped with dynamically changeable tools in order to realistically simulate different tools by providing appropriate contact cues to their users [8], [9]. Basically, when a user needs to interact with a specific tool in a specific pose, the robot fetches the appropriate tool and moves to the correct site presenting a highly realistic bare hand haptic experience. Combining this technology with a fully immersive head mounted display (HMD) means that virtual contents that match the training scenario can be seamlessly presented—the user cannot observe the robotic device. We argue that these advantages make encountered-type HAV environments ideal for virtual training.

While previous work has demonstrated the value of encountered-type haptic displays for tasks such as juggling [7] or manipulating an automobile control panel [8], these works use simulations in relatively small areas—those that fit within the physical workspace of the robot. In contrast, many training scenarios require activity in relatively large workspaces—in

Manuscript received January 30, 2017; accepted June 15, 2017. Date of publication July 17, 2017; date of current version March 17, 2020. This work was supported by the Plant Research Program through the Ministry of Land, Infrastructure and Transport of Korean Government under Grant 14IFIP-B085984-04. This paper was recommended by Associate Editor Y. Hata. *(Corresponding author: Jeha Ryu.)*

C.-G. Lee is with the Department of Mechatronics, Human Robotics Laboratory, Gwangju Institute of Science and Technology, Gwangju 61005, South Korea (e-mail: chonenome@gmail.com).

G. L. Dunn and J. Ryu are with the School of Mechanical Engineering, Human Robotics Laboratory, Gwangju Institute of Science and Technology, Gwangju 61005, South Korea (e-mail: gldunn@gist.ac.kr; ryu@gist.ac.kr).

I. Oakley is with the School of Design and Human Engineering, Ulsan National Institute of Science and Technology, Ulsan 44919, South Korea (e-mail: ian.r.oakley@gmail.com).

Color versions of one or more of the figures in this paper are available online at http://ieeexplore.ieee.org.

Digital Object Identifier 10.1109/TSMC.2017.2719037

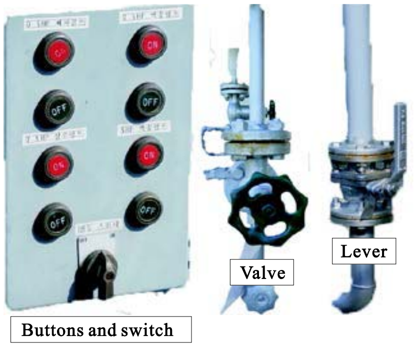

Fig. 1. Typical real tools (buttons, valves, and levers) in a plant facility.

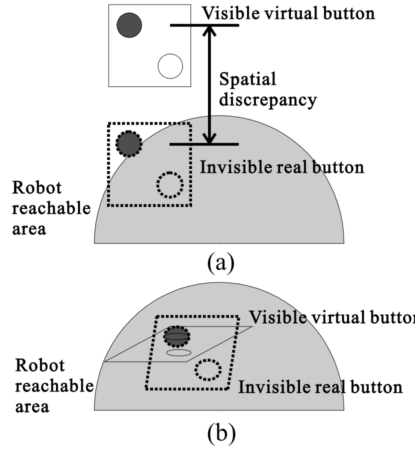

Fig. 2. Spatial discrepancy due to a pose difference. (a) Translational spatial discrepancy. (b) Roational spatial discrepancy.

the virtual plant scenario, for example, tools may be distributed over spaces that are several meters in size. It is infeasible, both mechanically, economically and in terms of safety, to deploy encountered-type haptic displays over such scales. This results in inevitable spatial discrepancies, or misalignments, between the physically constrained haptic and larger visual workspaces. This paper extends the authors' previous feasibility study of visual guidance [10] that seeks to address this problem through the design of a novel technique that dynamically manipulates the presented visual cue to align the workspaces and minimize the impact of spatial discrepancies.

This paper presents the following contributions. First, it defines the problem of spatial discrepancy for the encountered-type HAV environments. Second, it presents an algorithm using a technique we term visual guidance in order to resolve this problem. Third, it presents details of a design for a fully immersive encountered-type HAV system for training on the virtual plant simulation. Fourth, it presents two studies that evaluate the performance of the visual guidance of the HAV system. Using a typical button pressing task, the studies explore objective measures of performance (e.g., error rate and number of speed peaks) and whether or not the visual guidance algorithm influences simulator sickness (SS) ratings.

II. Spatial Discrepancy Problem and Solution Candidates

We define spatial discrepancy as *a mismatch in pose, size, or shape of a visually perceived object in the virtual world and a corresponding haptically perceived object in the real world*. For example, differences in position between a graphically presented model of a tool and its real-world haptic equivalent. Achieving minimal spatial discrepancy between modalities is an important aspect of creating a realistic haptic simulation. For example, research has shown it to be key to achieving feelings of presence in passive haptic applications [11] and for improving outcomes in haptic VR training systems [12].

Fig. 2 shows typical translational and rotational spatial discrepancies due to pose differences between virtual graphical contents and real physical buttons. In the context of an encountered-type haptic display these kinds of pose difference occur when a real button held by the robot cannot be positioned to match the pose of the virtual button due to, for example, limitations in the volume of its reachable workspace (illustrated as a shaded hemi-circle in Fig. 2). While such limits may be due to kinematic constraints, they can also be imposed to ensure trainee safety or stiff and robust haptic feedback [13]. This paper argues that this form of spatial discrepancy will occur commonly in encountered-type HAV systems and focuses on how to best accommodate these to create effective experiences for trainees.

Prior work has shown that spatial discrepancies negatively impact targeting performance in noncollocated visual haptic environments; discrepancies were associated with increases in both task completion time and absolute errors in spatial positioning [14]. Furthermore, we note that large spatial discrepancies may result in complete failures in tasks such as button pressing. For example, if substantial spatial discrepancies (say 50 mm) exceed the size of a real button (say 20 mm), then a trainee may be unable to press the button in the physical world, rendering the training system ineffective. In order to counter these effects, simulations must ensure accurate visual haptic colocation so that a visually perceived stimulus closely matches its haptically presented partner.

Prior authors have noted these problems and proposed solutions. In the following sections, we review two of the most prominent in detail: 1) redirected touching [12] and 2) haptic retargeting [11].

A. Redirected Touching

Redirected touching [12] is a technique that "*warps virtual space to map a variety of virtual objects onto a single real object*" [15]. For example, in the scenario of training in an aircraft cockpit shown on a fully immersive HMD, multiple virtual cockpits are mapped to a single physical prop via distorting the virtual space. This operates as follows, considering a movement along only a vertical direction for a simplification. First, as shown in Fig. 3(a) there is a spatial discrepancy (three vertical spatial intervals) between the real and virtual buttons due to a pose difference. A virtual hand must move five blocks to touch the virtual button [right of Fig. 3(a)] while a real hand must move two blocks for the real button [left of Fig. 3(a)].

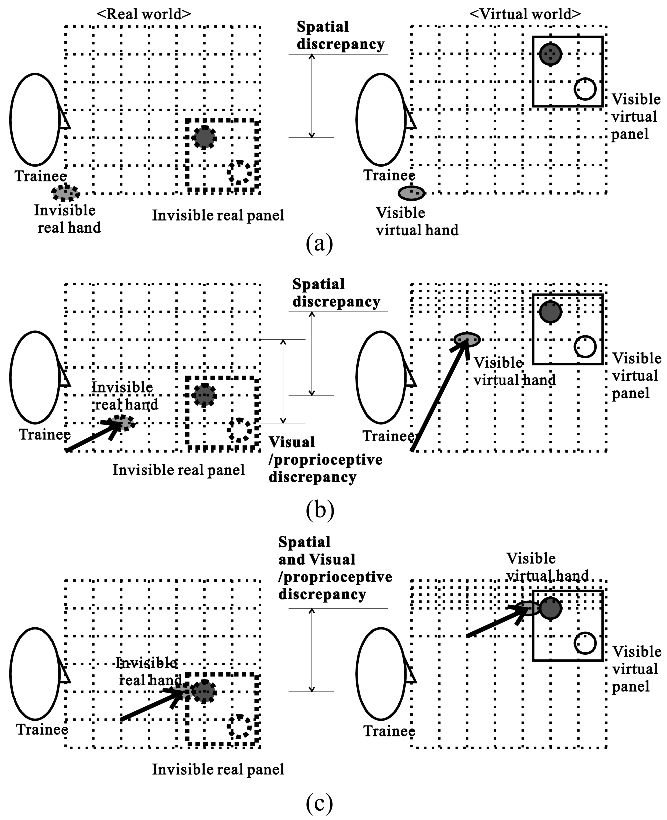

Fig. 3. How the redirected touching works. (a) Nonzero spatial discrepancy. (b) Hand reaching after virtual space warping. (c) Encountering real button after virtual space warping.

Therefore, the trainee cannot press the real button due to the three blocks difference. In order to resolve this problem, virtual space warping is performed [12]. As shown in Fig. 3(b), the real and virtual buttons are positioned at a distance of two blocks in vertical direction after the virtual space warping. In virtual world [right of Fig. 3(b)], the first spatial interval from the bottom is extended to be four times larger than the real world while the third–sixth spatial intervals are compressed four times smaller. As such, as shown in Fig. 3(b), a motion of one spatial interval in the up direction in the real world [left of Fig. 3(b)] results in four times larger motion in virtual world [right of Fig. 3(b)].

Although this technique ensures that both real and virtual hands come into contact with objects at the same time, it leads to substantial differences in visual and proprioceptive experiences of users: a proprioceptive distance moved does not match the visual presentation. We argue this sensory mismatch can be disturbing and impact performance or feelings of presence and, indeed, data supports this assertion. Studies of this technique [15] report that an adaptation to the warped virtual space and readaptation to the real world tasks both require substantial periods of training (e.g., 66 targeting trials) to mitigate performance degradation in a form of decreased throughput and increased error rate, task completion time, and trajectory variability.

There are further limitations to this technique in the context of encountered-type HAV environments. This boils down to the fact that spatial discrepancies in such systems will be harder to predict. Some virtual objects may exhibit zero spatial discrepancies as their physical instantiations remain within the reachable workspace of the robotic device. On the other hand, other virtual objects will be unreachable due to workspace limitations or factors such as safety considerations. This variability in the use of the technique will likely add to the cost it exerts in terms of user performance and training/retraining time. We argue this makes the technique a poor fit for encountered-type HAV systems.

B. Haptic Retargeting

As with redirected touching, haptic retargeting aims to reuse the passive haptics of a real object across multiple virtual objects [11]. It relies on the dominance of visual cues when senses conflict. Three variants were proposed: 1) world; 2) body; and 3) hybrid warping. In world warping, translations and rotations are applied to the entire virtual world in order to align in with the static pose of a real object. As with prior work on redirected walking [16], the required translations/rotations are presented to users as distortions of head movements. For example, if a virtual object is to the left of its physical counterpart, then head movements that precede actual reaching movements will be manipulated to incorporate exaggerated rightward rotations of the virtual world in order to align the two objects precisely. Body warping operates during reaching movements and is basically similar to redirected touching [12]. It includes extensions to dynamically detect targets and presents the whole hand (rather than just a finger) in the virtual space. Finally, hybrid warping combines these techniques, splitting the required warping between them.

The technique was compared during a task involving manipulation of three virtual cubes represented physically by one real cube. They revealed that the haptic retargeting improved the sense of presence when compared to typical wand-based 3-D control of virtual objects. Furthermore, hybrid warping achieved the higher satisfaction and presence scores than world and the body warping.

While promising, we note that the head rotations (that precede targeting movements) required for world and hybrid warping may occur infrequently in many cases involving relatively small spatial discrepancies between the virtual and real worlds—there may be little reason to adjust head position before performing a targeting task. As such, this requirement may make environments appear more unnatural. In addition, as with redirected touching, adaptation to the warped virtual space is necessary to perform tasks optimally using body or hybrid warping. Due to these problems, we argue that further research on alternative approaches to matching visual and haptic cues in the encountered-type HAVs is currently required.

III. Visual Guidance

This paper proposes a novel visual guidance algorithm to address spatial discrepancies between virtual visual and real haptic cues when using an encountered-type HAV. It operates based on a simple principle. If a spatial discrepancy

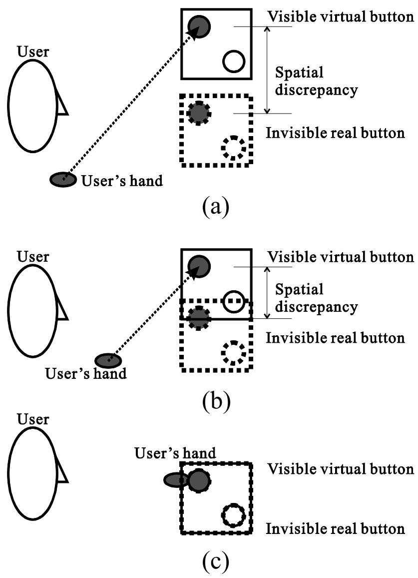

Fig. 4. Conceptual representation of the visual guidance. (a) Nonzero spatial discrepancy. (b) Decreasing spatial discrepancy. (c) Zero spatial discrepancy.

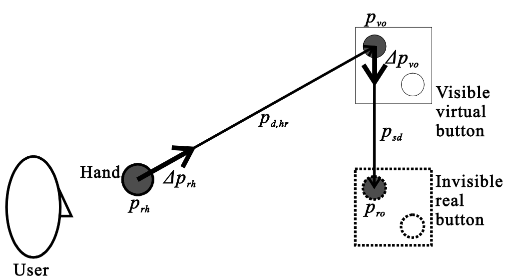

Fig. 5. Coordinate relationship for the visual guidance.

exists between real and virtual objects [e.g., buttons shown in Fig. 4(a)], the algorithm guides the user's hand to the real button by gradually translating and/or rotating the entire virtual scene including the virtual button to the pose of the real button *during the user's reaching motion*. This means that the virtual tool pose arrive at the real tool pose when the hand reaches the virtual tool at the same time. Fig. 4(a)–(c) illustrates this idea through a series of translational adjustments to the visible virtual button, which is displayed through a fully immersive HMD, until it matches the real physical button.

A. Steps in Visual Guidance

The following is a detailed step-by-step description of the visual guidance algorithm.

1) Obtain the amount of *pose (translation and rotation)* difference between the real and virtual tools from the robot internal sensors (e.g., by means of forward kinematics) and from the virtual environment, respectively. Spatial discrepancy values can then be computed for each ith degree-of-freedom component [note that Fig. 5 shows only the translational vector of $\boldsymbol{p}_{\mathrm{sd}}(t)$] as

$$P_{\mathrm{sd},i}(t) = P_{\mathrm{ro},i}(t) - P_{\mathrm{vo},i}(t) \tag{1}$$

where the capital letter $P_{\mathrm{ro},i}(t)$ and $P_{\mathrm{vo},i}(t)$ are the ith degree-of-freedom component for the real and virtual tool poses. Note that the ith degree-of-freedom represents either translational $(i = x, y, z)$ or rotational $(i = \theta, \emptyset, \varphi)$ motion, in which the rotation angles $(i = \theta, \emptyset, \varphi)$ may represent Euler angles or roll, pitch, yaw angles.

2) Obtain the amount of *position* difference between the trainee hand and virtual tools from the external tracker and from the virtual environment, respectively. Then compute the desired hand reach position vector $\boldsymbol{p}_{d,hr}(t)$ from the origin of the trainee hand to the origin of the virtual tool as:

$$\boldsymbol{p}_{d,hr}(t) = \boldsymbol{p}_{vo}(t) - \boldsymbol{p}_{\mathrm{rh}}(t) \tag{2}$$

where $\boldsymbol{p}_{vo}(t)$ and $\boldsymbol{p}_{\mathrm{rh}}(t)$ are the virtual object and real hand position vectors, respectively. Note in this step that only the translational degrees-of-freedom is used because a gradual change of the virtual object *pose (translation and rotation)* toward the real object *pose (translation and rotation)* can be computed by *a single time-varying proportional scalar* $c(t)$ in the next step.

3) In order to have the virtual tool pose arrive at the real tool pose when the hand reaches the virtual tool at the same time, the following relationship must be hold:

$$\frac{\left|\boldsymbol{p}_{d,hr}(t)\right|}{\left|\triangle\boldsymbol{p}_{d,hr}(t)\right|/\triangle t} = c(t) = \frac{P_{\mathrm{sd},i}(t)}{\triangle P_{\mathrm{sd},i}(t)/\triangle t} \tag{3}$$

where

$$\triangle\boldsymbol{p}_{d,hr}(t) = \boldsymbol{p}_{d,hr}(t) - \boldsymbol{p}_{d,hr}(t-1) \tag{4}$$

$$\triangle P_{\mathrm{sd},i}(t) = P_{\mathrm{sd},i}(t) - P_{\mathrm{sd},i}(t-1). \tag{5}$$

Then, from (3), the gradual pose change $\triangle P_{\mathrm{sd},i}(t)$ $(i = x, y, z, \theta, \emptyset, \varphi)$ during small time change $\triangle t$ must be inversely proportional to a proportional scalar $c(t)$ as

$$\triangle P_{\mathrm{sd},i}(t) = \frac{P_{\mathrm{sd},i}(t)}{c(t)} \times \triangle t. \tag{6}$$

From (1), $\triangle P_{\mathrm{sd},i}(t)$ can be represented as

$$\triangle P_{\mathrm{sd},i}(t) = \triangle P_{\mathrm{ro},i}(t) - \triangle P_{\mathrm{vo},i}(t), (i = x, y, z, \theta, \emptyset, \varphi) \tag{7}$$

where

$$\triangle P_{\mathrm{ro},i}(t) = P_{\mathrm{ro},i}(t) - P_{\mathrm{ro},i}(t-1) \tag{8}$$

$$\triangle P_{\mathrm{vo},i}(t) = P_{\mathrm{vo},i}(t) - P_{\mathrm{vo},i}(t-1). \tag{9}$$

From (6) and (7), we can determine the gradual change $(\triangle P_{\mathrm{vo},i})$ of the virtual tool toward the real tool as

$$\triangle P_{\mathrm{vo},i}(t) = \triangle P_{\mathrm{ro},i}(t) - \frac{P_{\mathrm{sd},i}(t)}{c(t)} \times \triangle t. \tag{10}$$

4) Compute next the current ith component value of the virtual tool pose by using (9) and (10) as

$$P_{\mathrm{vo},i}(t) = P_{\mathrm{vo},i}(t-1) + \triangle P_{\mathrm{ro},i}(t) - \frac{P_{\mathrm{sd},i}(t)}{c(t)} \times \triangle t. \tag{11}$$

At the final step of the algorithm, as shown in Fig. 4(c), the spatial and visual/proprioceptive discrepancies become or

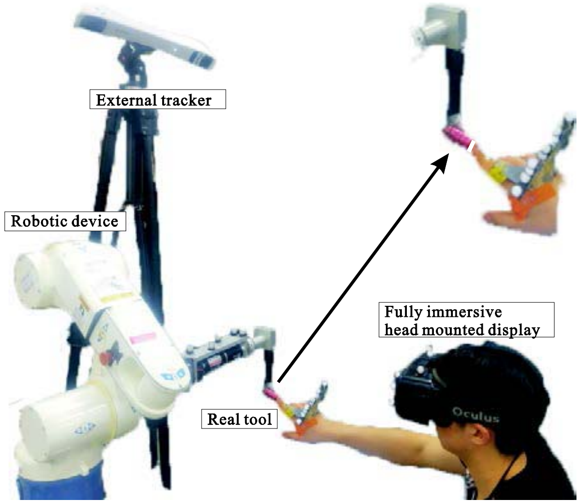

(a)

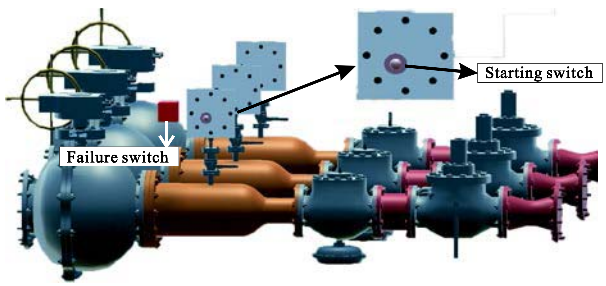

(b)

Fig. 6. Experimental setup. (a) Hardware configuration. (b) Virtual environment setup.

approximate zero. This means that both visual and haptic contact occur synchronously with spatial coincidence.

Comparing to the redirected touching and haptic retargeting algorithms that use virtual space warping, the proposed visual guidance has the following advantages. First, no visual/proprioceptive discrepancy occurs between the real and virtual hands because they are the same, i.e., they are moving together without any warping. Therefore, adapting the hand motion to the warped virtual space is not required. Second, since adjustments with the visual guidance occur during the hand reaching motion, head motions that precede targeting actions are no longer required, which may increase the fluidity and naturalness of interacting with the system.

IV. Validation of the Visual Guidance

In order to assess the effectiveness of the proposed visual guidance algorithm, this paper is modeled on that used to evaluate the related redirected touching algorithm [12]. The experimental details are described in this section.

A. Experimental Setup

Fig. 6(a) shows the experimental setup of our fully immersive HAV system. Participants stood (for the translational experiment) or sat (for the rotational experiment) in front of a robot. They wore a fully immersive HMD and a marker on their dominant hand for tracking purposes. We alternated between standing and sitting poses during the two experiments to balance different concerns. Basically, our experiments with seated participants removed or minimized confounds such as inevitable body/head motions that occur during standing. For example, a participant moving his or her head toward a virtual button during the experiments would result in a perceptibly larger target that, in turn, might result in a reduced objective measure of error rate. Because of this, a stable head motion should be enforced throughout the experiment. However, as described in Section III, the whole virtual scene moves during adaptions to translational spatial discrepancy. These movements may lead to postural instability and, ultimately, unfortunate events such as users falling. Assessing the extent of these undesirable results is also a crucial aspect of validating the visual guidance algorithm. These concerns led us to conduct our first experiment with standing participants (to assess postural stability) and our second experiment with seated participants (to minimize confounds).

During the experiments, participants were also asked to wear headphones to block audio cues from the robotic device. An HMD (Oculus Rift DK2 [17]) displayed virtual graphical content, while a button was mounted on a large-workspace robotic device (Denso robot arm, VS-6577G [18]) to display haptic cues. An external tracker (PST Iris [19]) with an optical marker system was used to acquire head and hand positions. The HMD provided a visual representation of a plant facility [Fig. 6(b)] and, based on data from the tracker (accurate to 0.5 mm and 1° with root mean square), the robotic device moved in order to present real buttons to the operator at system specified poses. The experiment was performed with respect to a complex virtual plant facility containing pipes, valves, and levers, and a button panel intended to resemble a real training situation. The panel featured eight buttons, each 20 mm in diameter and at equidistant angles apart (i.e., at cardinal and intercardinal angles). The button panel resembled that used in the study of redirected touching [12]. A single real button with a matching 20-mm diameter was attached to an end-effector of the robotic device to provide a realistic haptic experience of button pressing. We had the Denso robot arm move the real button prior to each trial in order to generate zero and nonzero spatial discrepancies on demand.

This setup achieved the practical requirements for studying spatial discrepancies in encountered-type haptic displays. These include the following.

1) Precise feedback control of a robotic device to generate a precise quantity of spatial discrepancy.
2) Precise sensing of a user's head to create accurate visual haptic collocated feedback (relative poses between user head and real tool and between virtual camera and virtual tool must coincide).
3) Precise sensing of a user's hand to apply accurate visual guidance.
4) Precise identification of button press events or failures to terminate a trial properly.

B. Experimental Conditions

The experiments were designed to validate the effectiveness of the visual guidance algorithm based on different levels of both translational and rotational spatial discrepancy.

To simplify the study design, translation and rotation were evaluated in separate experiments. To provide a fuller picture of the algorithm's performance, both experiments considered distortions in two spatial axes (translations in and rotations about x- and y-axis). However, to maintain the number of conditions at a manageable level, variations in each axis were considered separately rather than in a crossed design. This approach led to a large and diverse set of conditions that we believe represents a generalizable performance of the algorithm.

In the translational experiment, spatial discrepancy ranged from -150 to $+150$ mm with an increment of 50 mm along the two primary axes that formed a vertical plane in front of the participants (left/right and top/bottom). This generated six nonzero spatial discrepancy conditions for each axis and one zero spatial discrepancy condition (13 in total). We excluded the near/far axis from the experiment because movements on this axis would inherently alter travel distances during the trials and thus potentially confound measures such as task completion time.

The magnitudes of rotational spatial discrepancy varied from -40 to $+40°$ with an increment of 10° along the same two primary axes (left/right and top/bottom). This resulted in eight nonzero spatial discrepancy conditions for each axis and one zero spatial discrepancy condition (17 in total). This range of angles was chosen because the earlier study that evaluated redirected touching [12] examined spatial discrepancy up to 24° and showed effective performance up to 18°. We believe visual guidance may be effective at greater spatial discrepancies and thus selected a wider range. Finally, we excluded rotational spatial discrepancy around the near/far axis because button rotation in this dimension had no effect on the circular buttons used in the study.

C. Experimental Design

In order to explore systematically the effectiveness of visual guidance for accommodating genuine spatial discrepancies, misalignments were generated by translating or rotating the real button rather than its virtual counterpart. This movement occurred prior to each trial to ensure that the visual button locations were always identical and thus yielded no clue as to the level of spatial discrepancy being simulated in each trial.

Trials in both translational and rotational experiments were organized into blocks of eight trials, with each trial involving one button press on the control panel. During a single block, each button was pressed exactly once in a consistent order. Furthermore, both experiments were designed such that each spatial discrepancy was displayed on each button only once. To prevent practice or adaptation effects, the order in which spatial discrepancies were presented was fully randomized; in each block of eight trials, eight randomly selected spatial discrepancies were displayed, one on each of the eight buttons. In this manner, know what spatial discrepancy would be displayed from one trial to the next was impossible for the participants. The total number of trials in the translation experiment was 104 (six nonzero spatial discrepancies multiplied by two axes, plus one zero spatial discrepancy, and multiplied by eight buttons) and 136 in the rotation study (eight nonzero spatial discrepancies multiplied by two axes, plus one zero spatial discrepancy, and multiplied by eight buttons). Prior to each study, practice conditions were presented to participants. In both experiments, these conditions involved only three levels of spatial discrepancy (-50, 0, 50 mm, and $-20°$, 0°, 20°) and were thus presented in five blocks (40 trials). Training sessions lasted approximately 15 min, whereas main experiments lasted 45–60 min. Participants were enforced to take a break in both experiments after participants completed batches of four blocks. In addition, participants were free to take a break whenever they desired.

D. Measures

Dependent variables in these experiments were the failure rate of button press operations, the degree of smoothness of targeting paths taken by users to reach buttons, and user postural stability during the button presses. Failure rate was measured simply as the number of trials in which the target was missed (i.e., no button press occurred) over the total number of trials. The smoothness of the targeting paths was calculated only in successful trials and expressed as a number of speed peaks that is, spikes in speed that were both preceded and followed by lower values. We argue that this measure is a simple representation of path smoothness: quickly and accurately pressing a target button can be achieved in a single ballistic targeting motion with only one speed peak. However, if participants make trajectory corrections during the task, multiple separate ballistic movements and two or more speed peaks will be the result. This measure is fundamentally of the number of discrete targeting motions that occur in each trial and is important because the dynamic movements of the virtual scene generated by the visual guidance algorithm may disrupt the natural targeting behaviors of users and require them to produce more than one distinct movement. This measure captures these variations.

Finally, postural stability was assessed by recording the distance the participant's head moved during a trial [20]. This measure reflects the fact that postural instability relates to body motion, which is inevitably reflected in head motions. This measure is intended to verify whether the visual guidance algorithm generates postural instability [20]. The specific data captured was the aggregate head movement distance that occurred during each trial.

Additional measures to characterize movements included: average/peak speeds of hand motions and hand trajectory. Measures of speed may be reduced in cases when visual guidance is used, because it requires users to follow a gradually moving virtual tool. In this paper, hand trajectory was used to cast more light on the actual movements. This measures the path traveled by the user's hand during each trial.

E. Experimental Procedures

Each experiment began by providing an overview of the process to participants. This included a general description of the procedures and their expected duration. Participants were specifically informed that "during the experiment, the displayed contents might behave strangely." However, they were encouraged to "try to complete the task to the best of your abilities." No precise description of this "strange" behavior (the gradual movement of the virtual world caused by the visual guidance algorithm) was provided. We notified participants of this because, similar to redirected touching or haptic retargeting, the occurrence of somewhat unnatural behaviors in a virtual scene is inevitable when the visual guidance algorithm is employed. In these studies, advance warnings were used to reduce the number of questions about visual movements and prevent participants from halting their tasks. In this paper, we adopted this same strategy. Participants were also instructed that they could move their head back and forth, up and down, or left and right during a training session in order to reach toward the target button. However, they were asked to maintain stationary head and body positions as much as possible during the main experiment. This was necessary because the head was being tracked in order to reflect graphically the head's precise positions. Wide ranging head motion cause the distance and direction of buttons to change and were factors that could confound the experiment.

In each trial, participants were asked to move a fingertip, represented virtually as a spherical cursor, to a statically located "starting switch" displayed as a 30-mm diameter sphere [see Fig. 6(b)]. This starting switch then linearly expanded from 30 to 60 mm during the next two seconds. If the participants removed his or her finger from the switch during that period, it returned to its 30-mm initial state. After two seconds of contact, the starting switch disappeared and the trial began. This technique, adapted from a previous targeting study [14], was used to ensure a uniform start position for each trial and to minimize the impact of reaction time to the measures. In each trial, one button on the control panel was highlighted red and the participant was tasked with pressing button "as quickly and accurately as possible." Participants were told that if they failed to touch the real button, they should not manually search for it. Instead, they should remove their hand and touch the "failure switch" [see Fig. 6(b)] to indicate trial failure. Using the failure switch simplified the means of capturing the error rate. Each trial ended with the participant pressing either the target or failure switch. The subsequent trial then began immediately.

F. Experimental Results

Ten participants (eight males) aged 23–29 years [average: 26.3, standard deviation (SD): 1.73], all of whom were right-handed and had normal or corrected to normal vision, completed the study on translational spatial discrepancies. In addition, ten participants (nine males) aged 23 to 32 years old (average: 27.1, SD: 2.73), all of whom were right-handed and had normal or corrected to normal vision, completed the study on rotational spatial discrepancies.

Tables I–IV present the raw performance measures of error rate, the number of speed peaks, and distance of head motion with respect to the spatial discrepancies and primary axes. Upper and lower numbers in the tables denote means and standard errors, respectively. To explore the differences depicted in these tables, we ran two-way repeated measures analysis of variances (RM-ANOVAs) using the statistical package for the social sciences [21] for each dependent variable. In cases in which sphericity was violated, Greenhouse-Geisser corrections were applied. Tables V and VI show the results. Statistically significant differences existed among the spatial discrepancy levels in the translational experiment for the number of speed peaks and head motion distances. To understand this result, we analyzed this data using post-hoc pair-wise comparisons that incorporated Bonferroni confidence internal

TABLE I
PERFORMANCE MEASURES VERSUS TRANSLATIONAL SPATIAL DISCREPANCY

Spatial discrepancies / Measures	-150	-100	-50	0	50	100	150
Error rate	0.144 (0.025)	0.094 (0.027)	0.088 (0.028)	0.075 (0.033)	0.075 (0.022)	0.081 (0.028)	0.113 (0.033)
Number of speed peaks	1.286 (0.090)	1.173 (0.063)	1.131 (0.043)	1.077 (0.021)	1.189 (0.051)	1.175 (0.046)	1.284 (0.061)
Distance of head motion (m)	0.049 (0.006)	0.047 (0.005)	0.040 (0.005)	0.041 (0.007)	0.041 (0.006)	0.040 (0.006)	0.042 (0.006)

TABLE II
PERFORMANCE MEASURES VERSUS PRIMARY AXIS FOR TRANSLATIONAL DISCREPANCY

Spatial discrepancies / Measures	Left / right	Top / bottom
Error rate	0.093 (0.024)	0.098 (0.020)
Number of speed peaks	1.192 (0.038)	1.184 (0.037)
Distance of head motion (m)	0.043 (0.006)	0.043 (0.005)

TABLE III
PERFORMANCE MEASURES VERSUS ROTATIONAL SPATIAL DISCREPANCY

Spatial discrepancies / Measures	-40	-30	-20	-10	0	10	20	30	40
Error rate	0.094 (0.023)	0.050 (0.016)	0.031 (0.014)	0.038 (0.014)	0.038 (0.019)	0.063 (0.019)	0.069 (0.020)	0.094 (0.033)	0.094 (0.035)
Number of speed peaks	1.315 (0.089)	1.252 (0.069)	1.267 (0.057)	1.255 (0.051)	1.261 (0.057)	1.321 (0.062)	1.285 (0.057)	1.248 (0.042)	1.262 (0.049)

TABLE IV
PERFORMANCE MEASURES VERSUS PRIMARY AXIS FOR ROTATIONAL DISCREPANCY

Spatial discrepancies / Measures	Left / right	Top / bottom
Error rate	0.064 (0.022)	0.063 (0.012)
Number of speed peaks	1.261 (0.045)	1.287 (0.048)

TABLE V
STATISTICAL ANALYSIS FOR MAIN AND INTERACTION EFFECTS WITH TRANSLATIONAL SPATIAL DISCREPANCY

Variables / Measurements	Spatial discrepancy	Axis	Spatial discrepancy * Axis
Error rate	$F(6, 54) = 1.375$, $p=0.241$, $\eta_p^2=0.133$	$F(1,9)=0.135$, $p=0.722$, $\eta_p^2=0.015$	$F(2.496,22.468)=0.247$, $p=0.828$, $\eta_p^2=0.027$
Number of velocity peaks	$F(6, 54) = 2.383$, **$p=0.041$***, $\eta_p^2=0.209$	$F(1,9)=0.076$, $p=0.789$, $\eta_p^2=0.008$	$F(2.081,18.732)=0.198$, $p=0.830$, $\eta_p^2=0.022$
Distance of head motion	$F(6, 54) = 4.731$, **$p=0.001$*****, $\eta_p^2=0.345$	$F(1,9)=0.977$, $p=0.349$, $\eta_p^2=0.098$	$F(2.757,24.817)=0.989$, $p=0.408$, $\eta_p^2=0.099$

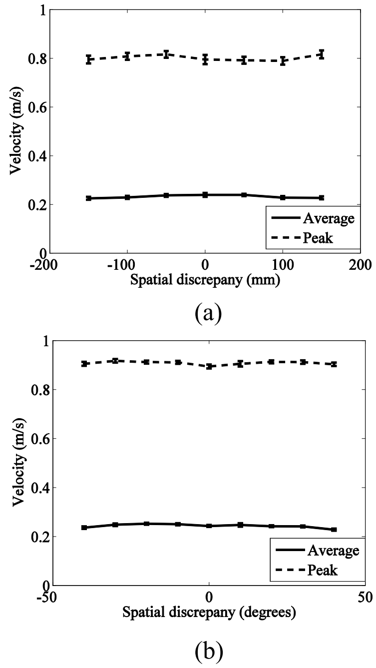

Fig. 7. Velocities versus spatial discrepancy. (a) For translational spatial discrepancy. (b) For rotational spatial discrepancy.

adjustments. Because the main purpose of this paper was to identify differences between nonzero and zero spatial discrepancies, we focused on only these comparisons. For error rate, none achieved significance. Except for the comparison involving spatial discrepancies of 100 mm ($p = 0.724$) and 150 mm ($p = 0.331$), all comparisons produced $p = 1$. Similarly, for head motion distance, no comparisons attained significance and, excepting the comparison involving a spatial discrepancy of -150 mm ($p = 0.175$), all produced $p = 1$. To provide a more nuanced picture of the differences, the effect sizes in the form of Cohen's [22] d were computed and are shown in Table VII for dependent variables that achieved statistically significant RM-ANOVA results.

For a fuller description of the experimental data, Figs. 7 and 8 present average and peak speeds as well as representative hand trajectories for each spatial discrepancy. In Fig. 8, the data represented are examples of trajectories from a single participant for each spatial discrepancy, and does not represent aggregate results. Fig. 8(a) and (b) represents hand trajectories when a button was placed on the right and left sides of the starting position, respectively.

Finally, visual guidance moved the virtual tool (and, effectively, the whole virtual scene) at speeds of 0.0336, 0.0634, and 0.0868 m/s during trials with 50-, 100-, and 150-mm spatial discrepancy, respectively. Note that the speed at which the virtual tool moved was not arbitrarily determined. It was based on the speed of the hand moving toward the target, which was deemed natural in terms of visual guidance. Nevertheless, error rates of zero and nonzero spatial discrepancies produced statistically nonsignificant results. This suggests that, within this range of movement speeds, visual guidance effectively mitigates the spatial discrepancy problem.

TABLE VI
STATISTICAL ANALYSIS FOR MAIN AND INTERACTION EFFECTS WITH ROTATIONAL SPATIAL DISCREPANCY

Measurements \ Variables	Spatial discrepancy	Axis	Spatial discrepancy * Axis
Error rate	$F(3.630, 32.669) = 1.909$, $p = 0.138$, $\eta_p^2 = 0.175$	$F(1, 9) = 0.005$, $p = 0.948$, $\eta_p^2 = 0.001$	$F(8, 72) = 2.000$, $p = 0.058$, $\eta_p^2 = 0.182$
Number of velocity peaks	$F(3.647, 32.822) = 0.425$, $p = 0.773$, $\eta_p^2 = 0.045$	$F(1, 9) = 2.186$, $p = 0.173$, $\eta_p^2 = 0.195$	$F(3.710, 33.391) = 1.181$, $p = 0.336$, $\eta_p^2 = 0.116$

TABLE VII
COHEN'S d FOR THE NUMBER OF SPEED PEAKS AND THE DISTANCE OF HEAD MOTION WITH RESPECT TO SPATIAL DISCREPANCY VARIATIONS

Measurements \ Spatial discrepancy	-150	-100	-50	50	100	150
Number of velocity peaks	0.727	0.590	0.447	0.774	0.725	**1.258**
Distance of head motion	0.410	0.310	0.039	0.004	0.034	0.036

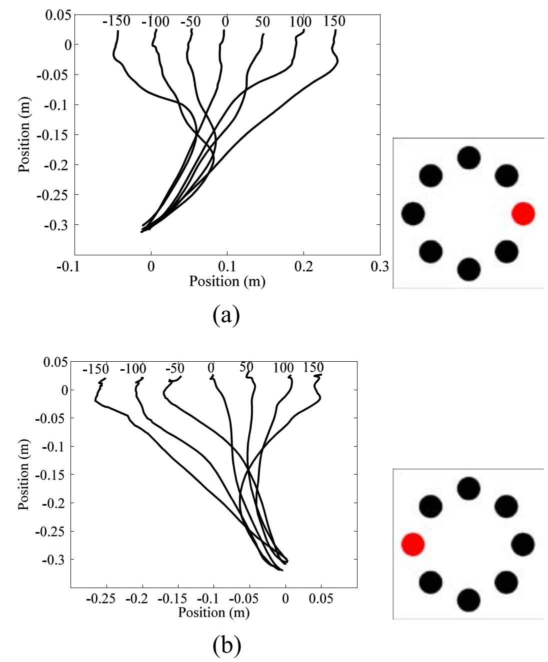

Fig. 8. Hand trajectories for every spatial discrepancy (top view). With a specific button at the (a) right side of the start position and (b) left side of the start position.

G. Discussion

In the main measures of error rate and number of speed peaks, only a single significant difference was observed: the error rate varies significantly with different spatial discrepancies. The minimum recorded error rate was 3.8% with zero spatial discrepancy and the maximum was 16.9% with a -150-mm spatial discrepancy. Although the former rate is typical of good performance in normal experimental settings, the latter is sufficiently high to raise doubts about the reliability of the technique with these extreme spatial discrepancy settings. Basically, the data suggest that error rates may increase as spatial discrepancies increase and that the visual guidance algorithm is required to make more substantial adjustments to the visual contents. The data also suggest that sensible working limits for the algorithm may be within 150 mm. However, it is worth noting that both relatively low effect size and lack of significant post-hoc tests indicate the current data are insufficient for the visual guidance algorithm to be effective to a statistically verifiable limit.

It is worth discussing the effect size data in detail. As seen in Table VII, effect sizes for the number of speed peaks fall in the moderate to high range, suggesting differences in the number of separate ballistic motions in the discrepant conditions, even if these did not generally attain significance. By contrast, in the measure of head movement distance, effect sizes range from very minor to moderate (for extreme −150-mm spatial discrepancy). This suggests that participant head movements were stable when the spatial discrepancy conditions were applied. This result suggests that visual guidance did not lead to postural instability, despite its use of scene manipulations. We believe this is because postural instabilities are typically induced by prolonged (e.g., 5 min) exposure to oscillating and/or random scene movements [20]. However, visual guidance involves virtual scene manipulations that are short (a few seconds) and neither random nor oscillating. These differences account for the lack of postural stability problems with the visual guidance algorithm.

Tables II and IV show the impact of the direction of visual guidance on task performance. As shown, slight differences exist that do not yield significant results. Therefore, we conclude that the direction in which visual guidance occurs does not impact task performance.

The lack of significant differences generally supports the idea that the visual guidance algorithm is effective. In a wide range of conditions involving spatial discrepancies of various translations and rotations, the system was able to guide a user to the target button as effectively as when no spatial discrepancy was present. This result highly validates the algorithm: the algorithm enabled participants to move to their destination targets in single, smooth, and accurate motions. This is also borne out by the data presented in Figs. 7 and 8. Average and peak velocities are higher than those reported in previous studies [14], [23] and static across different spatial discrepancies. The actual targeting paths in Fig. 8 are relatively smooth and direct, thus indicating that participants followed the target accurately as it moved based on adjustments specified by the visual guidance algorithm. In Fig. 8, note that the initial directions of hand motions are toward the visual target. For example, a target on the right side of the starting position [shown in the right side of Fig. 8(a)] results in an initial motion toward the right. Similarly, if a target is displayed on the left [see the hand trajectories on the left side of Fig. 8(b)], initial movements will be toward the left.

Comparing our results with those reported by previous authors of related work is also necessary. We argue that visual guidance offers improvements over redirected touching because users have greater errors with the redirected touching before they have sufficiently adapted to the system or been fully trained. Visual guidance can be used immediately without this problem occurring. In addition, visual guidance results in fewer errors than in redirected touching after users have adapted to the system. Specifically, this paper reveals an error rate of less than 10% with 40° spatial discrepancies, whereas redirected touching generated an error rate greater than 15% with discrepancies of only 24°.

This paper also suggests that visual guidance is simpler regarding both its ease of implementation and computational cost at run time. As described in Section III, the steps to achieve visual guidance involve a simple, linear geometric relationship between the hand and the real and virtual tools. By contrast, redirected touching involves a more complicated design (a thin-plate spline [24]) to achieve virtual space warping. Similarly, to achieve the most effective hybrid warping approach in haptic retargeting, additional complexity in present in the sensing system: that is the movements of the hand, head, and both real and virtual tools must be tracked. With visual guidance, the head need not be tracked. Accordingly, we argue that visual guidance is easier to implement than are previous approaches.

This paper has several limitations. First, as previously mentioned, our experiments did not include a crossed design for spatial discrepancy along the two primary axes. Instead, each axis was examined in turn. This allowed us to consider a wider range of single axis spatial discrepancies without a combinatorial explosion in the number of conditions. We argue that the lack of significant differences observed in the experiments validates this choice. Because no differences were observed with spatial discrepancies on a single axis, we suggest that these differences are unlikely to emerge with similar spatial discrepancies involving two axes. Nevertheless, exploring this issue empirically would be valuable in a follow-up study.

Second, our experiments focused on buttons, which are perhaps the simplest tools that could be deployed. The effect of visual guidance with more complex tools requires further study. Despite this limitation, we believe the current results are meaningful because previous studies on redirected touching also tested rotational spatial discrepancy using buttons [12], [15].

Finally, while data derived from out two experiments validate the quantitative objective performance of the visual guidance algorithm, subjective concerns are also critical to address. Specifically, we suggest that gradual movements of the visual scene caused by the visual guidance algorithm during a reaching motion may cause increased feelings of SS due to sensory conflict between the moving visual scene and static proprioceptive perceptions [25]. In order to address this issue, we conducted a follow-up study, which is described in the following section.

V. Subjective Evaluation of Visual Guidance

In order to assess whether the visual guidance algorithm increases SS, we conducted two short experiments involving trials with zero spatial discrepancy and the most extreme spatial discrepancies previously considered (150 mm and 40°). We assessed SS using the SS questionnaire (SSQ) [26], which is a 16-item concerning about participants' current body condition. For each item, participants evaluated their body condition based on a four item scale: 1) none; 2) slight; 3) moderate; and

TABLE VIII
RESULTS OF STATISTICAL ANALYSIS WITH PAIRED t-TEST BETWEEN NONE AND THE VISUAL GUIDANCE

	Nausea	Oculomotor	Disorientation	Total score
Translation	t(10) = 2.390 **p = 0.038***	t(10) = 1.649 p = 0.130	t(10) = 0.384 p = 0.709	t(10) = 1.391 p = 0.194
Rotation	t(10) = 1.401 p = 0.191	t(10) = 1.483 p = 0.169	t(10) = 0.671 p = 0.517	t(10) = 1.506 p = 0.163

4) severe. With participant answers and a predefined weighting table, we computed ratings for constructs of "nausea," "oculomotor," "disorientation," and "total score." By sampling participants at different times, we could track and compare their levels of SS through an experiment [27].

In the two experiments described here, each participant completed two blocks of button pressing tasks: one with zero and one with maximum (150-mm translational or 40° rotational) spatial discrepancy. They completed four SSQs, one before and after each block of the tasks. Calculating the delta between construct scores on pretest and post-test questionnaires allowed us to derive a measure of the change in SS resulting from performance of a task. In this manner, we could verify whether the visual guidance generated increased levels of SS by comparing changes in the four measures after zero and maximum spatial discrepancy tasks were completed. We used a single block of trials in these experiments as sustained activation of the visual guidance is not a typical use scenario. We anticipate that the experiment would need to be deployed sporadically, such as for a few minutes per hour, during a typical training task. We also opted to contrast zero spatial discrepancy with the maximum levels we previously studied because this represents an extreme case: that is, it involves the largest movements of a virtual scene and is thus most likely to increase SS. Each block of trials in the experiments required approximately five minutes to complete; we also enforced a break of 5 min between each block to allow participants to recover from any SS. The presentation order of the blocks was balanced among participants; half started with zero spatial discrepancy and finished with the maximum, whereas the other half did the reverse.

Eleven participants completed each experiment. The translational study included five males and six females with a mean age of 32.36 (SD: 14.34), whereas the rotational study included three males and eight females with a mean age of 30.55 (SD: 10.91). Fig. 9 shows the results of these experiments. The data were normalized with respect to maximum possible values for each construct (nausea: 200.34, oculomotor: 159.18, disorientation: 292.32, and SSQ total score: 235.62). Error bars in Fig. 9 denote standard error.

The data indicate that all four constructs increased after all study tasks were performed. The increases after conditions of spatial discrepancy were modestly greater than those following tasks with conditions without spatial discrepancy. This suggests that the visual guidance may increase SS. In order to verify whether this difference was significant statistically, a series of paired t-tests were performed. Table VIII shows the results of these tests. A statistically significant difference appeared only for the nausea construct in the translational experiment. All other conditions and constructs

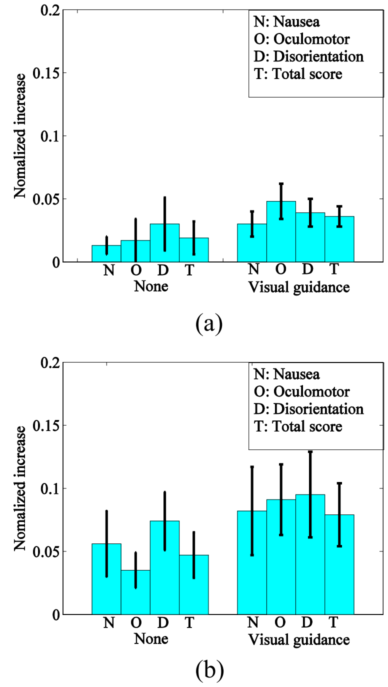

Fig. 9. Results of subjective evaluation by using the SSQ. (a) Translational spatial discrepancy. (b) Rotational spatial discrepancy.

led to nonsignificant results, suggesting that the visual guidance algorithm led to feelings of SS comparable to those experienced under normal virtual environment interaction. In general, we interpret this result positively. Specifically, although we noted an increase in nausea with a large spatial discrepancy, in general, the visual guidance algorithm did not significantly increase SS.

VI. CONCLUSION

This paper described the manner in which spatial discrepancies may occur as a result of pose differences between real and virtual tools in an HAV environment using an encountered-type haptic display. It proposed a technique known as visual guidance to mitigate degraded performance caused by these spatial discrepancies. Experiments verified the effectiveness of visual guidance with both translational and rotational spatial discrepancies along primary axes by measuring the error rate, number of speed peaks, and distance of head motion. The results revealed that the technique allows participants to smoothly and reliably press a target button when it included up to 150-mm translational and 40° rotational spatial discrepancies with postural stability. Additionally, participants' paths of motion remained similar regardless of the spatial discrepancy present; average and peak speeds were comparable across all experiments. Participants performed tasks without having to adapt to the system, suggesting that the visual guidance can be used without dedicated training. Finally, follow-up experiments suggested the technique yields only modest increases to SS when spatial discrepancies are large. Based on these experimental results, we conclude that visual guidance is a useful technique that can be applied to HAV environments that use an encountered-type haptic display.

Future research will examine visual guidance with rotational spatial discrepancies when users operate more complex tools such as valves or levers. The rotational motion of these tools during reaching is more complex than for the simple form of a button and may result in degraded performance with even small spatial discrepancies. An additional topic for future research is to consider spatial discrepancies resulting from size or shape mismatches. By considering these diverse scenarios, we hope to provide a useful technique that can increase the value and usefulness of encountered-type HAVs.

REFERENCES

[1] T. R. Coles, D. Meglan, and N. W. John, "The role of haptics in medical training simulators: A survey of the state of the art," *IEEE Trans. Haptics*, vol. 4, no. 1, pp. 51–66, Jan./Mar. 2011.

[2] M. Wurpts, "Poster: Updating an obsolete trainer using passive haptics and pressure sensors," presented at the 3D User Interfaces, Lafayette, LA, USA, Mar. 2009, pp. 155–156.

[3] F. Hu *et al.*, "Cyberphysical system with virtual reality for intelligent motion recognition and training," *IEEE Trans. Syst., Man, Cybern., Syst.*, vol. 47, no. 2, pp. 347–363, Feb. 2017.

[4] J. Huang, X. Tu, and J. He, "Design and evaluation of the RUPERT wearable upper extremity exoskeleton robot for clinical and in-home therapies," *IEEE Trans. Syst., Man, Cybern., Syst.*, vol. 46, no. 7, pp. 926–935, Jul. 2016.

[5] P. Milgram, H. Takemura, A. Utsumi, and F. Kishino, "Augmented reality: A class of displays on the reality-virtuality continuum," in *Proc. SPIE Telemanipulator Telepresence Technol.*, Dec. 1995, pp. 282–292.

[6] Y. Yokokohji, R. L. Hollis, and T. Kanade, "WYSIWYF display: A visual/haptic interface to virtual environment," *Presence Teleoper. Virtual Environ.*, vol. 8, no. 4, pp. 412–434, Aug. 1999.

[7] P. Tripicchio, E. Ruffaldi, C. A. Avizzano, and M. Bergamasco, "Control strategies and perception effects in co-located and large workspace dynamical encountered haptics," presented at the EuroHaptics Conf., Salt Lake City, UT, USA, Mar. 2009, pp. 63–68.

[8] M. Yafune and Y. Yokokohji, "Haptically rendering different switches arranged on a virtual control panel by using an encountered-type haptic device," presented at the World Haptics Conf., Istanbul, Turkey, Jun. 2011, pp. 551–556.

[9] S. Kim, S.-Y. Baek, and J. Ryu, "Development of haptic-robotic platform for virtual plant safety operation training," presented at the Int. Conf. Mechatronics Inf. Technol., Pattaya, Thailand, Dec. 2015, pp. 123–126.

[10] C.-G. Lee, G. L. Dunn, I. Oakley, and J. Ryu, "Visual guidance for encountered type haptic display: A feasibility study," presented at IEEE Int. Symp. Mixed Augmented Reality, Sep. 2016, pp. 74–76.

[11] M. Azmandian, M. Hancock, H. Benko, E. Ofek, and A. D. Wilson, "Haptic retargeting: Dynamic repurposing of passive haptics for enhanced virtual reality experiences," in *Proc. CHI Conf. Human Factors Comput. Syst.*, San Jose, CA, USA, May 2016, pp. 1968–1979.

[12] L. Kohli, M. C. Whitton, and F. P. Brooks, "Redirected touching: The effect of warping space on task performance," presented at the IEEE Symp. 3D User Interfaces, Costa Mesa, CA, USA, Mar. 2012, pp. 105–112.

[13] J.-P. Kim, S.-Y. Baek, and J. Ryu, "A force bounding approach for multi-degree-of-freedom haptic interaction," *IEEE/ASME Trans. Mechatronics*, vol. 20, no. 3, pp. 1193–1203, Jun. 2015.

[14] C.-G. Lee, I. Oakley, E.-S. Kim, and J. Ryu, "Impact of visual-haptic spatial discrepancy on targeting performance," *IEEE Trans. Syst., Man, Cybern., Syst.*, vol. 46, no. 8, pp. 1098–1108, Aug. 2015.

[15] L. Kohli, M. C. Whitton, and F. P. Brooks, "Redirected touching: Training and adaptation in warped virtual spaces," presented at the IEEE Symp. 3D User Interfaces, Orlando, FL, USA, Mar. 2013, pp. 79–86.

[16] S. Razzaque, Z. Kohn, and M. C. Whitton, "Redirected walking," presented at the Eurograph., 2001, pp. 289–294.

[17] Accessed on Jul. 3, 2017. [Online]. Available: https://www.oculus.com/en-us/dk2

[18] Accessed on Jan. 30, 2017. [Online]. Available: http://densorobotics.com/products/vs-g-series

[19] Accessed on Jul. 3, 2017. [Online]. Available: http://www.ps-tech.com/optical-trackers/optical-tracker-pst-iris

[20] S. J. Villard, M. B. Flanagan, G. M. Albanese, and T. A. Stoffregen, "Postural instability and motion sickness in a virtual moving room," *Human Factors Ergonom. Soc.*, vol. 50, no. 2, pp. 332–345, 2008.

[21] Accessed on Jul. 3, 2017. [Online]. Available: www.ibm.com/software/analytics/spss/

[22] J. Cohen, *Statistical Power Analysis for the Behavioral Sciences*. New York, NY, USA: Academic Press, 2013.

[23] M. A. Zahariev and C. L. MacKenzie, "Grasping at 'thin air': Multimodal contact cues for reaching and grasping," *Exp. Brain Res.*, vol. 180, no. 1, pp. 69–84, Jun. 2007.

[24] R. R. Saboo, "Atlas diffeomorphisms via object models," Ph.D. dissertation, Dept. Comput. Sci., Univ. North Carolina at Chapel Hill, Chapel Hill, NC, USA, 2011.

[25] R. H. Y. So, A. Ho, and W. T. Lo, "A metric to quantify virtual scene movement for the study of cybersickness: Definition, implementation, and verification," *Presence Teleoper. Virtual Environ.*, vol. 10, no. 2, pp. 193–215, Apr. 2001.

[26] R. S. Kenedy, N. E. Lane, K. S. Berbaum, and M. G. Lilienthal, "Simulator sickness questionnaire: An enhanced method for quantifying simulator sickness," *Int. J. Aviation Psychol.*, vol. 3, no. 3, pp. 203–220, 1993.

[27] B.-C. Min, S.-C. Chun, Y.-K. Min, and K. Sakamoto, "Psychophysiological evaluation of simulator sickness evoked by a graphic simulator," *Appl. Ergonom.*, vol. 35, no. 6, pp. 549–556, Nov. 2004.

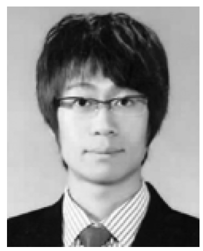

Chang-Gyu Lee received the B.S. degree from the Department of Mechanical Engineering, Chonnam National University, Gwangju, South Korea, in 2008, and the M.S. degree from the School of Mechatronics, Gwangju Institute of Science and Technology, Gwangju, in 2010, where he is currently pursuing the Ph.D. degree with the School of Mechatronics.

His current research interests include haptic training in virtual environment, haptic rendering, and haptic control stability.

Gregory Lynn Dunn received the B.S. degree in computer system science from Michigan Technological University, Houghton, MI, USA, in 2013. He is currently pursuing the master's degree with the Mechanical Engineering Department, Gwangju Institute of Science and Technology, Gwangju, South Korea.

His current research interests include haptic rendering, haptic modeling, and human response to multimodal virtual reality.

Ian Oakley received the B.S. degree (joint Hons.) from the Schools of Computing Science and Psychology, University of Glasgow, Glasgow, U.K., in 1998, and the Ph.D. degree from the School of Computing Science, University of Glasgow, in 2003.

He is an Associate Professor with the School of Design and Human Engineering, Ulsan National Institute of Science and Technology, Ulsan, South Korea. He has published over 80 research articles and reports. His current research interests include human–computer interaction and, specifically, in the areas of multimodal, physical, tangible, and social computing.

Prof. Oakley is a member of ACM SIGCHI.

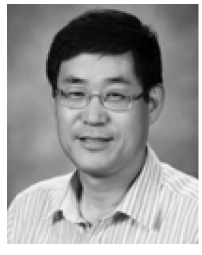

Jeha Ryu (M'03) received the B.S. degree from the Department of Mechanical Engineering, Seoul National University, Seoul, South Korea, in 1982, the M.S. degree from the Department of Mechanical Engineering, Korea Advanced Institute of Science and Technology, Daejeon, South Korea, in 1984, and the Ph.D. degree from the Department of Mechanical Engineering, University of Iowa, Iowa City, IA, USA, in 1991.

He is a Professor with the School of Mechatronics, Gwangju Institute of Science and Technology, Gwangju, South Korea. He has published over 200 research articles and reports. His current research interests include haptic interaction control, haptic modeling and rendering, haptic application for various multimedia systems, and teleoperation.